Effects of Shear Flow on Viscoelastic Properties of Polystyrene/Poly(vinyl methyl ether) Blends near the Phase Separation Temperature

Yoshiaki Takahashi,*,† Hirokazu Suzuki,‡ Yoshiki Nakagawa,§ and Ichiro Noda†

Department of Applied Chemistry, Nagoya University, Chikusa-ku, Nagoya 464-01, Japan, Central Research Laboratories, Kuraray Company, Ltd., 2045-1, Sakuzu, Kurashiki, Okayama 710, Japan, and Sumitomo Rubber Industries, Ltd., 1-1, 1-chome, Tsutsui-cho, Chuo-ku, Kobe 651, Japan

Received February 18, 1994; Revised Manuscript Received August 4, 1994®

ABSTRACT: Viscoelastic properties of polystyrene/poly(vinyl methyl ether) blends with nearly critical compositions were measured under steady-shear flows near the phase separation temperatures. In the homogeneous region, shear rate dependences of shear viscosity η and shear compliance J_S are practically the same as those of homopolymers. In the phase-separated region at quiescence, on the other hand, η and J_S are enhanced at low shear rates, but they become almost the same as those in the homogeneous region when the shear rates are higher than their respective critical shear rates. The critical shear rate values from J_S, $\dot{\gamma}_{cJ}$, were found to be larger than those from η, $\dot{\gamma}_{cV}$, and $\dot{\gamma}_{cJ}$ is considered to be almost equal to the critical shear rate for shear-induced homogenization $\dot{\gamma}_c$. Moreover, it was pointed out that, when $\dot{\gamma}_{cV}$ is smaller than the critical shear rate for non-Newtonian behavior of η, there exists a plateau region in the shear rate dependence of η.

Introduction

Theoretical and experimental studies on the effects of flow field on the phase separation behavior of polymer blends have been carried out extensively,[1-15] and they were recently summarized by Larson.[16] Most of the experimental studies can be classified into two categories. One is the scattering experiments in flow field, in which light scattering[6-8] or small-angle neutron scattering (SANS)[9,10] techniques were used to observe the phase separation or homogenization induced by flow. The other is the rheological experiments, in which the changes in the viscoelastic properties due to the phase separation or homogenization induced by flow were measured.[11-14]

It is worth discussing the results from the two kinds of studies together to understand the effects of flow on the phase separation behavior. However, these works have been usually carried out independently, and also there are too many parameters to be specified in both experiments.[10] Therefore, it is difficult to compare the results in the two kinds of studies so far published independently.

Recently, Nakatani et al.[10] studied the phase separation of a deuterated polystyrene/poly(vinyl methyl ether) (PSD/PVME) blend with the critical composition in steady shear flow by SANS. They observed the shear-induced homogenization. Moreover, they reported different shear rate dependences of shear viscosity η for the PSD/PVME blend and an ordinary polystyrene (PS)/PVME blend in the phase-separated region at quiescence. For the former, η decreased with an increase of $\dot{\gamma}$, similar to shear-thinning behavior observed in homopolymer systems. For the latter, η had a plateau region in the middle range of $\dot{\gamma}$ where the flow-induced homogenization was observed through a quartz window.

In a previous paper,[14] we reported viscoelastic properties of a PS/PVME blend (designated sample B1 in this work) of which the molecular weights and compositions are almost the same as those of the PS/PVME blend of Nakatani et al.,[10] over a wide range of temperature. In the phase-separated region at quiescence, we also observed that η had a narrow plateau region in the middle range of shear rate when the difference between experimental and phase separation temperatures was small. When the temperature difference was large, on the other hand, the plateau disappeared and the shear rate dependence of η became similar to that of the PSD/PVME system of Nakatani et al.[10]

During these measurements we observed that sample B1 in cone–plates became clear at high shear rates. This may indicate the occurrence of shear-induced homogenization. The η values in the plateau region are on the extrapolated line of the zero-shear viscosity vs temperature curve obtained in the homogeneous region for sample B1. This means that the η values in the plateau region of sample B1 are almost the same as the zero-shear viscosities η^0 of the homogenized state at the measured temperatures. Though the η data at the large temperature difference show shear-thinning behavior similar to that of homopolymer systems as mentioned above, the constant value of viscosity at low shear rate is not on the extrapolated line of the zero-shear viscosity vs temperature curve.

From the above results, it can be pointed out that the shear rate dependence of η in the phase-separated region at quiescence is complicated particularly when shear flows induce homogenization. Despite many works,[1,11-16] the viscoelastic properties of polymer blends including the above-complicated viscosity behavior are not yet elucidated.

According to Onuki,[3] it is predicted that, in the phase-separated region of near-critical fluids, the primary normal stress difference is a few orders of magnitude larger than that in the homogeneous region and it is proportional to shear rate. He also noted that the idea should be applicable to other systems which contain domain structures, such as immiscible polymer mixtures. Doi and Ohta[17] proposed a rheological theory for binary mixtures of immiscible fluids in which the proportionality of primary normal stress

† Nagoya University.
‡ Kuraray Co., Ltd.
§ Sumitomo Rubber Industries, Ltd.
® Abstract published in *Advance ACS Abstracts*, September 15, 1994.

0024-9297/94/2227-6476$04.50/0

Table 1. Molecular Characteristics of PS and PVME Samples

sample code	M_w	M_w/M_n
PS		
F20	1.9×10^5	1.04
F40	$3.5_5 \times 10^5$	1.02
PVME		
F6-4-2	4.0×10^4	1.24
F5-1	$9.0_9 \times 10^4$	1.40
NIST	$1.8_1 \times 10^5$	1.25

Table 2. Characteristics of Blend Samples

sample	PS	PVME	PS:PVME	T_C (°C)	T_S (°C)
B1	F20	F6-4-2	1:4	98	
B2	F40	NIST	1:4	107	
B3	F20	F5-1	1:4	87	88.2
B4	F20	F5-1	1:9	87.6	91.1
B5	F20	F5-1	3:7	87.5	88.3

difference to shear rate is also predicted. We have studied viscoelastic properties of binary mixtures of immiscible Newtonian fluids[18] and immiscible polymers[19] and reported that the primary normal stress differences are enhanced and their shear rate dependences are close to first power of shear rate, entirely different from those of components, whereas the viscosity and its shear rate dependence are not significantly different from those of components.

These results suggest that the effect of phase separation is more pronounced on primary normal stress difference than shear stress under steady shear flows. In this paper, therefore, we study the shear rate dependences of viscoelastic properties of PS/PVME blends including the samples with almost the same molecular weights and compositions as PS/PVME and PSD/PVME samples used by Nakatani et al.[10] near the phase separation temperature. The critical shear rate for shear-induced homogenization is determined from the shear rate dependence of primary normal stress data, and then the complicated viscosity behavior mentioned above is discussed in terms of the critical shear rate.

Experimental Section

Samples. PS samples used were purchased from Tosoh Co., Ltd. One of the PVME samples, which is the same as that used in the SANS experiments,[10] was kindly supplied by National Institute of Standards and Technology. This sample was precipitated in *n*-hexane to remove low molecular weight tails and characterized by the same method as used for other PVME samples. The other PVME samples purchased from Polysciences Inc. were fractionated in a mixture of benzene and *n*-hexane. Details of the fractionation and characterization of PVME samples were already reported.[20] The molecular characteristics of PS and PVME samples are listed in Table 1.

Homogeneous and transparent blend samples were prepared by freeze-drying the uniform benzene solutions of blend samples, followed by drying *in vacuo* at about 80 °C for 1 to a few days. The combinations of PS and PVME for blend samples are listed in Table 2. Samples B1, used in a previous work,[14] and B2 correspond to the PS/PVME and PSD/PVME samples, respectively, used by Nakatani et al.[10] Samples B3, B4, and B5 were prepared by using the same PS as in B1, but the molecular weight of PVME is between those in B1 and B2 and the compositions are slightly different.

Measurements of Phase Separation Temperature. Cloud points of polymer blend samples at zero heating rate were determined by measuring the transmitted intensity of a He–Ne laser through a 0.2-mm-thick sample film as reported previously.[14] In addition, scattered intensities of the laser beam were measured at three different angles for B3, B4, B5, and the blends of the same PS and PVME with other compositions. The scattering intensities at the zero heating rate were smoothly extrapolated to zero angle to determine the spinodal temperature. The cloud points T_{Cl} and spinodal temperatures T_S thus determined are also tabulated in Table 2. Only T_{Cl} was measured for samples B1 and B2 since these blends have the critical composition,[10,21] so that their T_{Cl}'s are very close to the T_S's or the critical points T_C.

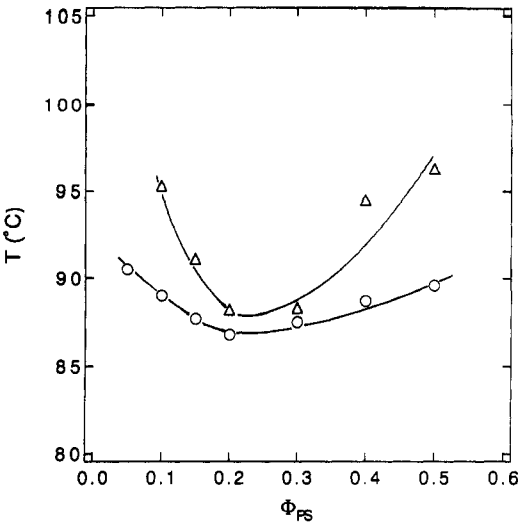

Figure 1. Phase diagram of the PS(F20)/PVME(F5-1) blend. Circles and triangles denote cloud points and spinodal temperatures, respectively.

Figure 1 shows the phase diagram of PS(F20) and PVME-(F5-1), having the lower critical solution temperature as reported in the literature.[21] The figure indicates that the volume fraction of PS, ϕ_{ps}, for B3 is close to the critical composition. Hereafter, we call the temperature regions where the samples are homogeneous and phase-separated at quiescence one-phase and two-phase regions, respectively.

Viscoelastic Measurements. The blend samples were molded to disks with a hot press at temperatures below T_{Cl} to prepare bubble-free specimens. Viscoelastic properties of blend samples were measured under steady shear flows with a Mechanical spectrometer Type RMS 800 of Rheometrics Co., equipped with the cone and plate geometry of 2.5 cm diameter and 0.1 rad cone angle. Dry nitrogen gas was used in the temperature control system of RMS 800 to avoid sample degradation and adsorption of moisture.

In the two-phase region, the samples were preheated to temperatures slightly below their T_{Cl} and then heated to measuring temperatures. The measurements were started 10 min after the measuring temperatures were reached.

Results

Shear Viscosity. Figure 2 shows double-logarithmic plots of shear viscosity η against shear rate $\dot{\gamma}$ in the one-phase region. The shear rate dependences of all the samples in the one-phase region are similar to those of homopolymers,[22] the viscosities are independent of shear rate at low shear rates, but they decrease with increasing the shear rate at high shear rates. Therefore, we can determine the zero-shear viscosity η^0 for all the samples at each temperature.

Figure 3 shows double-logarithmic plots of η against $\dot{\gamma}$ in the two-phase regions. The shear rate dependences of η in the two-phase region are different for different samples and temperatures. The shear rate dependences of η for sample B2 at 110 °C and B3 at 90 °C are almost the same as those in the one-phase region. For sample B4 there exists a narrow plateau region in the middle range of shear rate, as observed for sample B1, reported in a previous work.[14] For sample B5 the shear rate dependencies in high and low shear rate ranges are different. The same tendency can be seen for sample B2 at 119 °C.

Figure 4 shows temperature dependences of η^0 in the

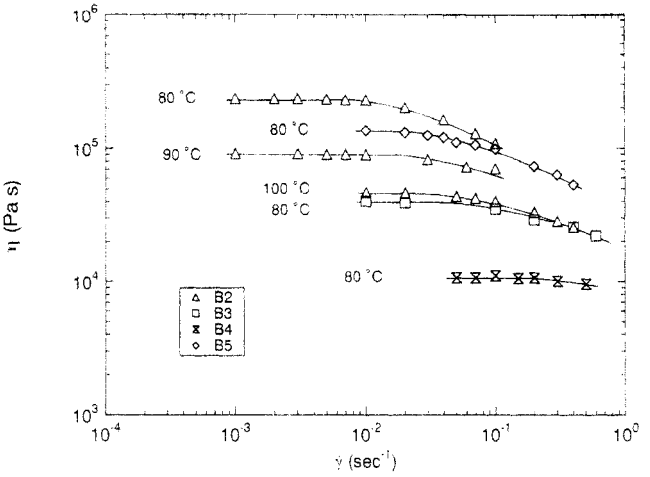

Figure 2. Double-logarithmic plots of shear viscosity η against shear rate $\dot{\gamma}$ for blend samples in the one-phase region. Symbols and temperatures are indicated in the figure.

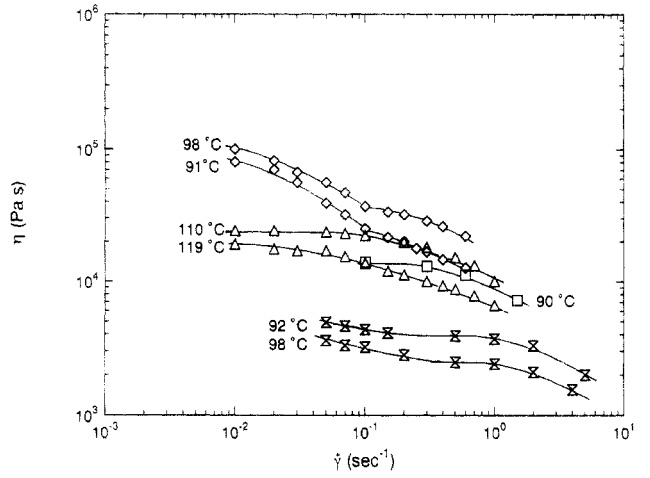

Figure 3. Double-logarithmic plots of shear viscosity η against shear rate $\dot{\gamma}$ in the two-phase region. Symbols are the same as in Figure 2. Temperatures are indicated in the figure.

one-phase region determined in Figure 2 and of η^0 for B1 in the one-phase region reported previously.[14] Since the shear rate dependences of primary normal stress difference as well as viscosity for sample B2 at 110 °C and B3 at 90 °C are the same as those in the one-phase region as shown later, we also evaluated η^0 values for these samples by extrapolating the data in Figure 3 at zero-shear rate and plotted them in this figure. Moreover, the plateau values of η for B1 and B4 in the two-phase region are plotted in this figure for comparison. Apparently, the viscosity data are connected by a smooth line for each sample, which seems to be parallel to each other, suggesting that the temperature shift factors a_T for these samples are the same.

Figure 5 shows plots of log a_T against T^{-1} obtained from Figure 4, where the reference temperature is 80.6 °C. The solid line denotes the shift factor for the PVME homopolymer as reported previously.[20] The temperature dependence of a_T for blend samples is almost the same as that of the PVME homopolymer. As pointed out in a previous paper,[14] it can be concluded that the free volumes or local frictional coefficients of the blend samples are mainly determined by PVME in these PVME-rich blends. As shown in Figures 4 and 5, the η^0 and a_T data evaluated in the two-phase region are consistent with the data in the one-phase region when shear rate dependences of viscosity and primary normal stress difference are the same as those in the one-phase region (B2 at 110 °C and B3 at 90 °C) and when the plateau appeared (B1 at 105 and 110 °C and

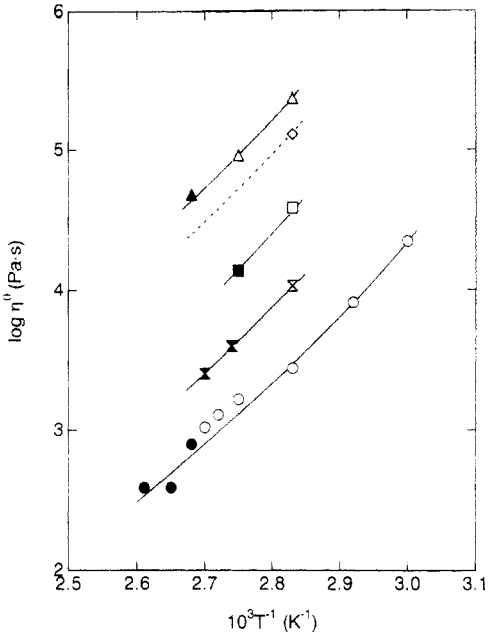

Figure 4. Plots of log η^0 against T^{-1}. Circles denote the data for sample B1. Other symbols are the same as in Figure 2. Open and filled symbols denote the data obtained in the one- and two-phase regions, respectively.

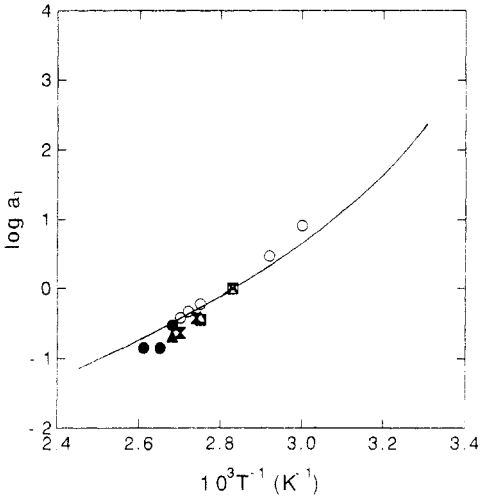

Figure 5. Plots of log a_T against T^{-1}. The reference temperature is 80.6 °C. Symbols are the same as in Figure 4. A solid line denotes data of the PVME homopolymer.[15]

B4 at 92 and 98 °C). This result implies that shear flows induce homogenization, though the complete homogenization cannot be determined by viscosity data only, as discussed later.

As mentioned above, the shear rate dependence of η in the one-phase region is similar to that of homopolymers. It is well-known for homopolymers that the master curve for shear viscosity can be obtained by plotting η/η^0 against $\dot{\gamma}/\dot{\gamma}_0$, where $\dot{\gamma}_0$ is defined as the shear rate at which $\eta = 0.8\eta^0$.[22] Double-logarithmic plots of η/η^0 against $\dot{\gamma}/\dot{\gamma}_0$ for the blend samples in the one-phase region are shown in Figure 6. Clearly, all the data compose a single master curve like homopolymers.

Primary Normal Stress Difference. Figure 7 shows double-logarithmic plots of primary normal stress difference $P_{11}-P_{22}$ against shear rate $\dot{\gamma}$ in the one-phase region. The shear rate dependences of $P_{11}-P_{22}$ for all the samples in the one-phase regions are similar to those of homopolymers,[23] $P_{11}-P_{22}$ are proportional to $\dot{\gamma}^2$ at low shear rates, but the shear rate dependence becomes lower with increasing shear rate, though the range where $P_{11}-P_{22} \propto$

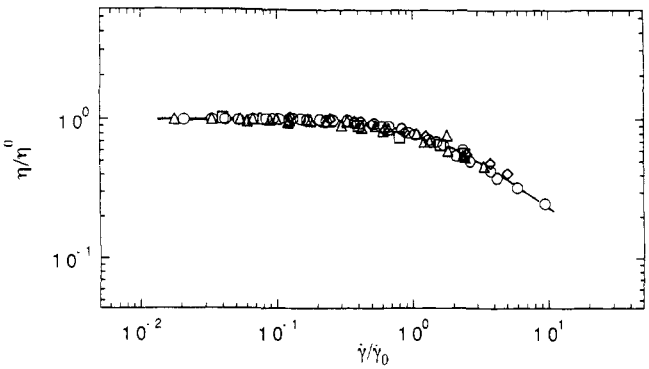

Figure 6. Master curve of reduced shear viscosity η/η^0 against reduced shear rate $\dot{\gamma}/\dot{\gamma}_0$ in the one-phase region. Symbols are the same as in Figure 4.

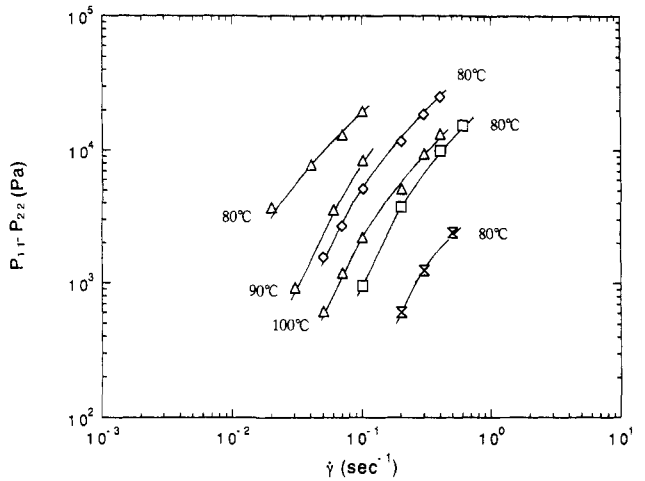

Figure 7. Double-logarithmic plots of primary normal stress difference $P_{11} - P_{22}$ against shear rate $\dot{\gamma}$ in the one-phase region. Symbols are the same as in Figure 2. Temperatures are indicated in the figure.

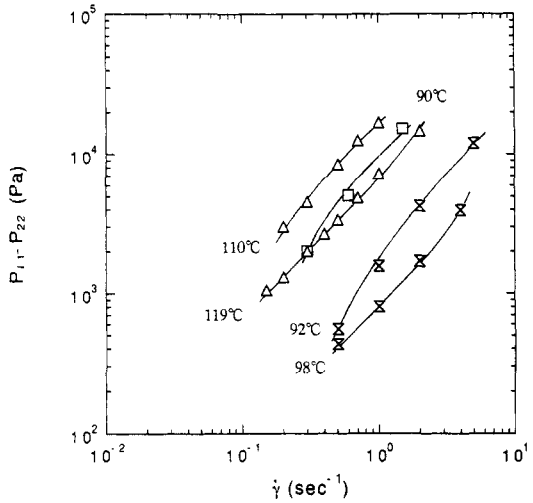

Figure 8. Double-logarithmic plots of primary normal stress difference $P_{11} - P_{22}$ against shear rate $\dot{\gamma}$ in the two-phase region. Symbols are the same as in Figure 2. Temperatures are indicated in the figure.

$\dot{\gamma}^2$ is narrow and the normal stress cannot be measured in the low shear rate range in comparison with shear stress.

Figure 8 shows double-logarithmic plots of $P_{11} - P_{22}$ against $\dot{\gamma}$ in the two-phase regions. $P_{11} - P_{22}$ for B1 and B5 in the two-phase region was not measured because of low normal stress at high temperatures. The shear rate dependence of $P_{11} - P_{22}$ in the two-phase region is different for different samples and temperatures as those of viscosity. In analogy with viscosity, the shear rate

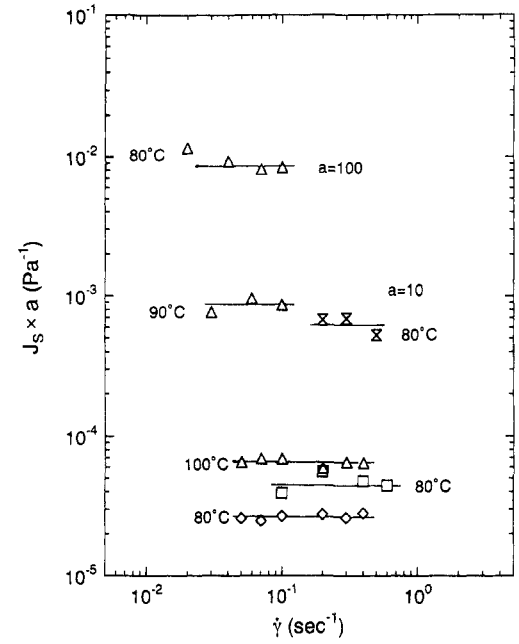

Figure 9. Double-logarithmic plots of shear compliance J_S against shear rate $\dot{\gamma}$ in the one-phase region. Symbols are the same as in Figure 2. Temperatures are indicated in the figure. The data for B2 at 80 °C are vertically shifted in 2 decades, while the two data for B2 at 90 °C and B4 at 80 °C are vertically shifted in 1 decade to avoid overlapping.

dependences of $P_{11} - P_{22}$ for samples B2 at 110 °C, B3 at 90 °C, and B4 at 92 °C are the same as those in the one-phase region. For B2 and B4 at higher temperatures (119 and 98 °C, respectively), $P_{11} - P_{22}$ is proportional to $\dot{\gamma}$ at low shear rates, but the shear rate dependence becomes slightly steeper at the higher shear rates.

In homopolymer systems, the elastic properties are usually discussed in terms of shear compliance $J_s = (P_{11} - P_{22})/2P_{12}^2$, where P_{12} is shear stress.[22,24] Similarly, we discuss the elastic properties of blend samples in terms of J_s. Figures 9 and 10 show double-logarithmic plots of J_s against $\dot{\gamma}$ in the one- and two-phase regions, respectively. In these figures some data are vertically shifted to avoid overlapping.

As shown in Figure 9, the J_s data in the one-phase region also resemble to those of homopolymers. At the measured shear rates J_s is almost constant for each sample at each temperature, so that the steady-state compliance J_e can be determined from these data in Figure 9. As shown in Figure 10, the shear rate dependence of J_s for samples B2 at 110 °C, B3 at 90 °C, and B4 at 92 °C is similar to that in the one-phase region so that J_e can also be obtained from these data. On the other hand, the J_s data for sample B2 at 119 °C and B4 at 98 °C decrease with increasing shear rate at low shear rates, but they become almost constant at high shear rates.

Figure 11 shows plots of log J_e against T^{-1}, determined from the data in Figures 9 and 10. Here, we also plotted the constant values of J_s data for sample B2 at 119 °C and B4 at 98 °C at high shear rates. All the data are multiplied by T/T_0 to reduce the temperature dependence,[22,24] though the temperature dependence of J_e is very small in the limited range of temperature similar to homopolymers. This result in Figure 11 implies that the constant values of J_s at high shear rates can be regarded as J_e of homogenized samples at those temperatures.

Discussion

In the two-phase region, the shear rate dependences of J_s (Figure 10) are rather simple compared to those of η

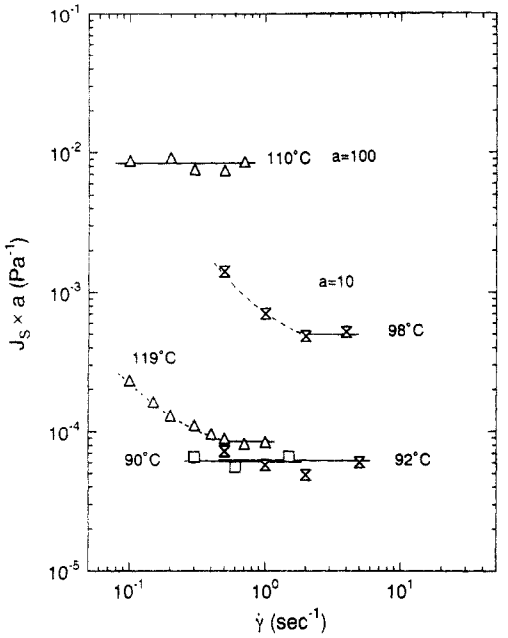

Figure 10. Double-logarithmic plots of shear compliance J_S against shear rate $\dot{\gamma}$ in the two-phase region. Symbols are the same as in Figure 2. Temperatures are denoted in the figure. The data for B2 at 110 °C are vertically shifted in 2 decades, while the data for B4 at 98 °C are vertically shifted in 1 decade to avoid overlapping.

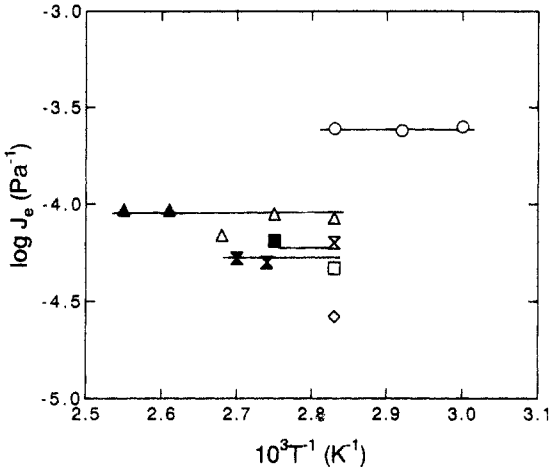

Figure 11. Plots of log J_e against T^{-1}. Symbols are the same as in Figure 2. Open and filled symbols denote the data obtained in the one- and two-phase regions, respectively.

(Figure 3) and can be classified into two cases in terms of experimental temperatures: (a) When ΔT_{CI} ($=T - T_{CI}$) is small (shallow quench), i.e., B2 at 110 °C, B3 at 90 °C, and B4 at 92 °C, J_s and its dependence on $\dot{\gamma}$ are consistent with the data in the one-phase region. (b) When ΔT_{CI} is large (deep quench), i.e., B2 at 119 °C and B4 at 98 °C, J_S decreases with an increase of $\dot{\gamma}$, reflecting $P_{11} - P_{22} \propto \dot{\gamma}$ at low $\dot{\gamma}$ region, but becomes constant at a critical shear rate $\dot{\gamma}_{cJ}$, reflecting the same shear rate dependence as in the one-phase region.

In case b the change from J_s behavior similar to binary mixtures of immiscible fluids to that of homogeneous polymers is obviously consistent with the theory for near-critical fluids.[3] That is, the large normal stress due to interfaces, which is proportional to shear rate, is obtained in the two-phase region, but it disappears when the system is homogenized and consequently the normal stress of the homogeneous polymer system is observed. Therefore, we consider that $\dot{\gamma}_{cJ}$ from these J_s data is almost equal to the critical shear rate for shear-induced homogenization $\dot{\gamma}_c$,

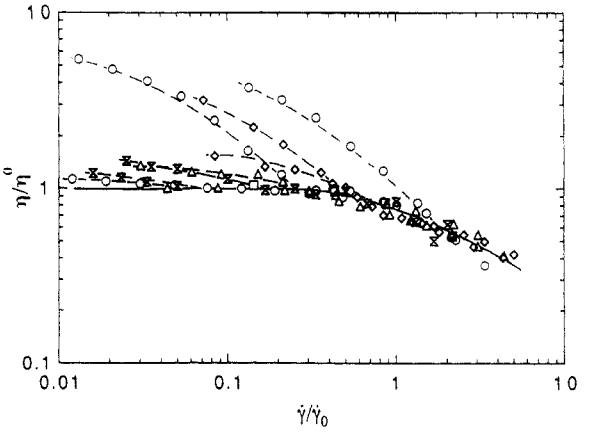

Figure 12. Superposition of reduced shear viscosity η/η^0 in the two-phase region. A solid line denotes the master curve in the one-phase region evaluated in Figure 6. Symbols are the same as in Figure 4.

though it should be confirmed by methods which can directly observe phase transition to get a definite conclusion.

The viscosity enhancement due to phase separation may also disappear around $\dot{\gamma}_{cJ}$. Thus we discuss the viscosity enhancement in terms of $\dot{\gamma}_{cJ}$ for the samples in which J_s data were measured, and then we discuss viscosity data for other samples in which J_s data were not measured. It should be noted that η can be measured at lower shear rates than J_s.

Since J_s of all the samples in case a is consistent with the data measured in the one-phase region, $\dot{\gamma}_{cJ}$ is lower than the measured shear rate of J_s in these cases. No viscosity enhancement is detected for B2 at 110 °C and B3 at 90 °C in the whole experimental range of shear rate. For sample B4 at 92 °C, on the other hand, small enhancement of viscosity due to phase separation is observed at the lower shear rate region where J_s was not measured. With an increase of shear rate, there exists a plateau region in η, in which η is consistent with η^0 in the one-phase region (Figure 4), so that a critical shear rate for disappearance of viscosity enhancement $\dot{\gamma}_{cV}$ can be determined. In this case the $\dot{\gamma}_{cV}$ value is slightly lower than the lowest measured shear rate for J_s, implying that the $\dot{\gamma}_{cV}$ is very close to $\dot{\gamma}_{cJ}$.

In case b there exists a plateau region for η of sample B4 at 98 °C, so that $\dot{\gamma}_{cV}$ can also be determined. It is apparent that $\dot{\gamma}_{cV}$ is lower than $\dot{\gamma}_{cJ}$ in this case. This result implies that the enhancements of η and J_s in the two-phase region disappear by shear flow at different shear rates; in other words, the $\dot{\gamma}_{cV}$ and $\dot{\gamma}_{cJ}$ values are not always the same. For sample B2 at 119 °C, no plateau is observed and viscosity continuously decreases with an increase of shear rate above and below $\dot{\gamma}_{cJ}$. In this case, we also speculate that the viscosity enhancement disappears at a certain value of $\dot{\gamma}_{cV}$ which is lower than $\dot{\gamma}_{cJ}$.

To examine the viscosity enhancement in more detail, all the viscosity data in Figure 3 were divided by η^0 at each temperature and the plots of η/η^0 data against $\dot{\gamma}$ were horizontally shifted so as to compose a master curve at high shear rates in Figure 12. Here, η^0 for B5 at 91 and 98 °C were evaluated according to the dotted line in Figure 4, which is drawn parallel to the solid lines for other data, while η^0 for B2 at 119 °C was evaluated by using the shift factor for PVME in Figure 5. For others, the data shown by filled symbols in Figure 4 were used. Apparently, the η/η^0 data for each sample at low shear rates are enhanced, but the data at high shear rates coincide with the master curve in the one-phase region shown by the solid line,

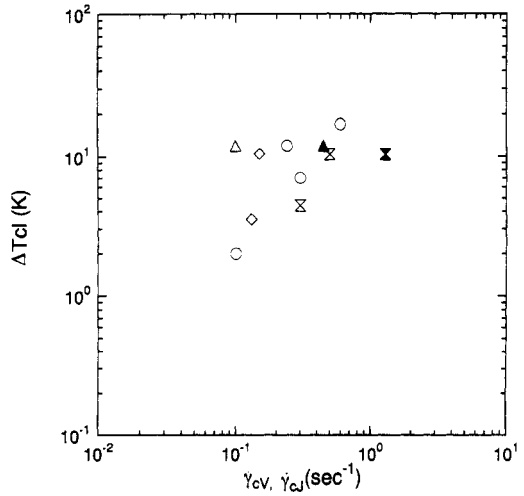

Figure 13. Double-logarithmic plots of ΔT_{Cl} against $\dot{\gamma}_{cV}$ and $\dot{\gamma}_{cJ}$. Symbols are the same as in Figure 4. Open and filled symbols denote $\dot{\gamma}_{cV}$ and $\dot{\gamma}_{cJ}$, respectively.

though they are somewhat scattered. Thus we can use this figure to determine the critical shear rate $\dot{\gamma}_{cV}$ for disappearance of viscosity enhancement as the shear rate at which η/η^0 merges into the master curve, even when the plateau is not observed in viscosity behavior. It should be noted that the viscosity enhancements smaller than $\eta/\eta^0 = 2$ were reproducible but large enhancements ($\eta/\eta^0 > 2$) observed in a few cases depended on the thermal history in the two-phase region.

The reason why a plateau is observed for shear viscosity in some cases but not in others can be understood by comparing $\dot{\gamma}_{cV}$ and a critical value of shear rates for non-Newtonian viscosity $\dot{\gamma}_0'$ where η starts to decrease from η^0. If $\dot{\gamma}_{cV} < \dot{\gamma}_0'$, the viscosity enhancement disappears before $\dot{\gamma}_0'$ so that the plateau appears, whereas if $\dot{\gamma}_{cV} > \dot{\gamma}_0'$, the viscosity enhancement still exists after $\dot{\gamma}_0'$ so that the plateau does not appear. If the system is homogenized by flow at $\dot{\gamma} < \dot{\gamma}_0'$, $\dot{\gamma}_0'$ is inversely proportional to the relaxation time of the homogenized blend. Even if the system is still phase-separated at $\dot{\gamma} > \dot{\gamma}_0'$, the compositions of the existing phases must be very close to that of the homogeneous state, so that $\dot{\gamma}_0'$ is also closely related to the inverse of the relaxation time of the homogenized blend.

Figure 13 shows double-logarithmic plots of ΔT_{Cl} against critical shear rates $\dot{\gamma}_{cV}$. It is clear that $\dot{\gamma}_{cV}$ are different for different molecular weights, compositions, and temperature; however, the difference in $\dot{\gamma}_{cV}$ is not significant in contrast to $\dot{\gamma}_0'$, which is inversly proportional to the product of $\eta^0 J_e$ and hence largely depends on molecular weights, compositions, and temperature.[25] The two filled symbols in Figure 13 show the critical shear rates $\dot{\gamma}_{cJ}$'s determined from J_s data of B2 at 119 °C and B4 at 98 °C (deep quench case). As already mentioned, $\dot{\gamma}_{cV}$ is smaller than $\dot{\gamma}_{cJ}$ when ΔT_{Cl} is large, but with decreasing ΔT_{Cl} the two critical shear rates become close to each other as observed for B4 at 92 °C. Therefore, for other samples of which J_s are not measurable, $\dot{\gamma}_{cV}$ are probably close to the real critical value for homogenization only when ΔT_{Cl} is small.

In summary, our conclusions are the following: (1) The shear rate dependence of $P_{11} - P_{22}$ in the two-phase region is the same as those for immiscible blends, and the change from $P_{11} - P_{22}$ or J_s behavior of immiscible blends to that of homogeneous polymers is distinctly observed in contrast to η, consistent with the theory for near-critical fluids[3], so that the critical shear rate for disappearance of enhancement of J_s, $\dot{\gamma}_{cJ}$, is considered to be almost equal to that for shear-induced homogenization, $\dot{\gamma}_c$. (2) The critical shear rates for the disappearance of enhancements of η and J_s, $\dot{\gamma}_{cV}$ and $\dot{\gamma}_{cJ}$, respectively, are close to each other in the shallow quench case, but the former is smaller than the latter in the deep quench case. (3) If $\dot{\gamma}_{cV}$ is smaller than a critical value of shear rates for non-Newtonian behavior of viscosity $\dot{\gamma}_0'$, the viscosity enhancement disappears before $\dot{\gamma}_0'$ so that the plateau appears in the shear rate dependence of η, whereas in the opposite case, the viscosity enhancement still exists after $\dot{\gamma}_0'$ so that the plateau does not appear.

Acknowledgment. This work was supported by a Grant-in-Aid for Scientific Research (No. 04453105) from the Ministry of Education, Science, and Culture of Japan.

References and Notes

(1) Utlacki, L. A. *Polymer Alloys and Blends*; Hanser Verlag: Munich, 1989.
(2) Doi, M.; Onuki, A. *Koubunnishi-Buturi Soteni Dynamics*; Iwanami: Tokyo, 1992.
(3) Onuki, A. *Phys. Rev. A* **1987**, *35*, 5149; *Int. J. Thermophys.* **1989**, *10*, 293.
(4) Pistoor, N.; Binder, K. *Colloid Polym. Sci.* **1988**, *266*, 132.
(5) Horst, R.; Wolf, B. A. *Macromolecules* **1993**, *26*, 5676.
(6) Takebe, T.; Sawaoka, R.; Hashimoto, T. *J. Chem. Phys.* **1989**, *91*, 4369.
(7) Hashimoto, T.; Takebe, T.; Asakawa, K. *Phys. A* **1993**, *194*, 338.
(8) Hindawi, I. A.; Higgins, J. S.; Weiss, R. A. *Polymer* **1992**, *33*, 2522.
(9) Nakatani, A. I.; Kim, H.; Takahashi, Y.; Han, C. C. *Polym. Commun.* **1989**, *30*, 143.
(10) Nakatani, A. I.; Kim, H.; Takahashi, Y.; Matsushita, Y.; Takano, A.; Bauer, B. J.; Han, C. C. *J. Chem. Phys.* **1990**, *93*, 795.
(11) Mazich, K. A.; Carr, S. H. *J. Appl. Phys.* **1983**, *54*, 5511.
(12) Ajji, A.; Choplin, L.; Prud'homme, R. E. *J. Polym. Sci., Part B* **1988**, *26*, 2279.
(13) Katsaros, J. D.; Malone, M. F.; Winter, H. H. *Polym. Eng. Sci.* **1989**, *29*, 1434.
(14) Takahashi, Y.; Suzuki, H.; Nakagawa, Y.; Noda, I. *Polym. Int.* **1994**, *34*, 327.
(15) Mani, S.; Malone, M. F.; Winter, H. H. *Macromolecules* **1992**, *25*, 5671.
(16) Larson, R. G. *Rheol. Acta* **1992**, *31*, 497.
(17) Doi, M.; Ohta, T. *J. Chem. Phys.* **1991**, *95*, 1242.
(18) Takahashi, Y.; Kurashima, N.; Noda, I.; Doi, M. *J. Rheol.* **1994**, *38*, 699.
(19) Takahashi, Y.; Kitade, S.; Kurashima, N.; Noda, I. *Polym. J. (Tokyo)*, accepted for publication.
(20) Takahashi, Y.; Suzuki, H.; Nakagawa, Y.; Noda, I. *Polym. J. (Tokyo)* **1991**, *23*, 1333.
(21) Nishi, T.; Wang, T. T.; Kwei, T. K. *Macromolecules* **1975**, *8*, 227.
(22) Graessley, W. W. *Adv. Polym. Sci.* **1974**, *16*, 1.
(23) Endo, H.; Fujimoto, T.; Nagasawa, M. *J. Polym. Sci., Polym. Phys. Ed.* **1970**, *9*, 375.
(24) Sakai, M.; Fujimoto, M.; Nagasawa, M. *Macromolecules* **1972**, *5*, 786.
(25) Watanabe, H.; Kotaka, T. *Macromolecules* **1987**, *20*, 530.